# NUMERICAL ANALYSIS OF POWER CONSUMPTION AND MIXING TIME FOR A PSEUDOPLASTIC LIQUID IN GEOMETRICALLY SIMILAR STIRRED VESSELS WITH SEVERAL KINDS OF PLATE-TYPE IMPELLERS

MEGURU KAMINOYAMA*[1], KAZUYOSHI ARAI*[2] AND MITSUO KAMIWANO
*Department of Material Science and Chemical Engineering, Yokohama National University, Yokohama 240*

***Key Words:*** Agitation, Numerical Analysis, Power Consumption, Mixing Time, Pseudoplastic Liquid, Scale-up

**A numerical analysis method of estimating power consumption for a pseudoplastic liquid in stirred vessels fitted with various plate impellers is first presented in terms of the energy dissipation distribution in the vessels. The pseudoplastic liquid used was a 1.2 wt.% aqueous solution of hydroxyethyl cellulose. Good agreement between numerically analysed results and experimental data of power consumption in a model vessel of 0.2 m diameter with various impellers and in a vessel of 0.4 m diameter with a paddle impeller proved the method to be sufficiently reliable. Subsequently, the same analysis and mixing analysis were numerically performed for geometrically similar large-scale vessels of 0.4, 0.6 and 0.8 m diameters. It was ascertained from these analyses that the relation between the scale-up ratio and the power consumption, mixing time, and mixing energy can be quantitatively estimated by a numerical analysis of stirred vessels with various types of stirring impellers for a pseudoplastic liquid.**

## Introduction

Estimation of the mixing power consumption by a pseudoplastic liquid is indispensable to the design of a reactor for a highly viscous non-Newtonian fluid, in which polymeric materials are produced. It is also decisive for optimum operation of the reactor to precisely estimate this value. The experimental method of drawing a power correlation diagram based on measurements of the shaft torque transmitted to the whole region of a stirred vessel[13, 15, 16, 18, 19] has been conventionally adopted for such evaluation. This approach, however, can never clarify how the power is locally consumed inside the vessel. In addition to, much laborious work is required to scale-up the stirred vessels when this approach is used. On the other hand, numerical analyses have been frequently attempted for a variety of phenomena in stirred vessels[1-10, 14, 17, 22-25] in the last decade. The authors *et al.* and some other investigators have reported on the numerical analysis method for fluid behaviour[2, 5, 7, 9] and the mixing process[8, 10, 24] for a pseudoplastic liquid in a stirred vessel. These analyses enable us to obtain the desired quantitative information throughout the vessel and to examine the scaling-up effect[9] readily under particular conditions. However, there are very few reports concerning the numerical analysis of power consumption in a non-Newtonian fluid in a stirred vessel, except those reported by Hiraoka *et al.*[5] and Bertrand *et al.*[2, 3]

In this study we first proposed a numerical analysis method for evaluating power consumption based on the results of a three-dimensional flow analysis of a pseudoplastic liquid in stirred vessels equipped with various kinds of plate-type impellers, and applied the method to model vessels of 0.2 m diameter at various rotational speeds of a stirring impeller. The reliability of the numerical analysis method was examined by comparison of the calculated results with the experimental data from a torquemeter. Subsequently, this analysis method was applied to geometrically similar large-scale vessels. Further, mixing energy, that is, the power required to attain mixing, was calculated in each scale vessel using the mixing time analyzed. We obtained the mixing time numerically from the mixing analysis method we previously proposed[8, 10].

The relation between scale-up ratio and power consumption, mixing time, and mixing energy in the stirred vessels for a pseudoplastic liquid was estimated from the analyses mentioned above for each shape of stirring impeller.

## 1. Numerical Analysis Method

### 1.1 Procedure of numerical analysis

1) Power consumption First we performed a three-dimensional flow analysis of a pseudoplastic liquid using the method[7] which we reported, that is, discretizing basic equations in a frame of the FDM and solving them by the simultaneous relaxation method for pressure and velocities. We can obtain from this analysis

*1) Received February 3, 1993. Correspondence concerning this article should be addressed to M. Kaminoyama.

*2) K. Arai is now with the Dept. of Industrial Eng. and Management, Nihon Univ., Narashino-city, Chiba 275.

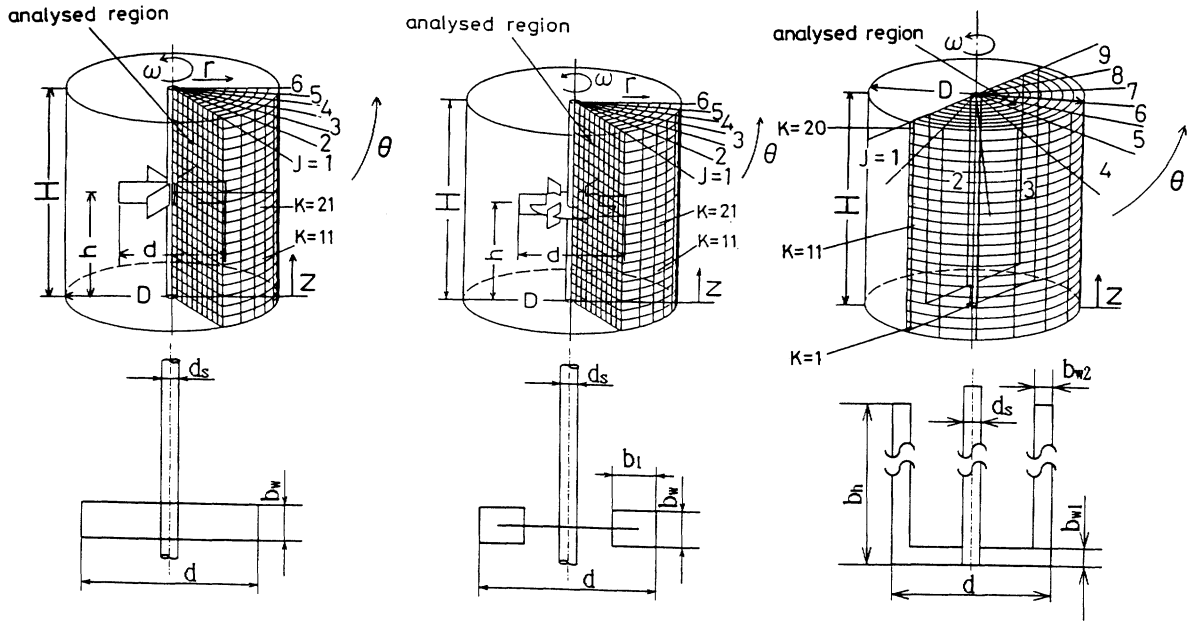


**Fig. 1** Schematic diagrams of stirred vessels fitted with: (a) paddle impeller; (b) turbine impeller; (c) anchor impeller

both distributions of the shear rate, $\dot{\gamma}$, and apparent viscosity, $\eta_a$, in each discretized mesh. The total power consumption in the vessel, $P$, can be calculated by the summation of energy consumed in each mesh throughout the vessel as shown in Eq. (1)[3, 21], assuming that the power supplied from outside the vessel is exclusively consumed as viscous dissipation of energy inside the vessel.

$$P = \sum_{I,J,K} [(\dot{\gamma}^2 \cdot \eta_a) \cdot \Delta V] \tag{1}$$

Where $I$, $J$, and $K$ indicate the number of each mesh divided into $r$, $\theta$, and $z$ directions, respectively, when we discretize the basic equations; $\dot{\gamma}$ is given by Eq. (2) using the second invariants of rate of the deformation tensor, $(\Delta : \Delta)$; and $\Delta V$ denotes the volume of each mesh.

$$\dot{\gamma} = (1/2(\Delta : \Delta))^{1/2} \tag{2}$$

The viscous dissipation of energy mentioned above is consumed as thermal energy to heat up the stirred liquid in a vessel. We, however, analyzed without heat transfer, because the increase in temperature is negligible under the conditions set in this study. We used the three-parameter power law model[26] given by Eq. (3) as a viscosity constitutive equation for a pseudoplastic liquid.

$$\eta_a = \frac{a}{1 + b(\dot{\gamma})^c} \tag{3}$$

2) Mixing time Mixing analysis[8, 10] was performed by numerically pursuing the dynamic change of solute concentration injected as a tracer at time 0 into a stirred pseudoplastic liquid flowing under steady state. The three-dimensional diffusion equation was numerically solved in a rotating coordinate system. The velocity vector obtained in the flow analysis mentioned above was applied to the convection terms on the assumption that the tracer shows the same behaviour as that of the mother liquid and that it does not affect the flow fields. The mixing time, $t_M$, is defined by the time when the degree of mixing attained, $M$, reaches 0.99. $M$ is evaluated as the ratio of the volume of the mixed region to the total volume, $V_{tot}$. The mixed region is given by the region where the dimensionless concentration, $C^*$, defined by Eq. (4) is less than 0.01.

$$C^* = \left| \frac{C - C_m}{C_0 - C_m} \right| \tag{4}$$

The mixing energy required for mixing attainment, $E_M$, can be estimated by the product of $P$ and $t_M$.

3) Scale-up criterion The criterion for the scale-up of stirred vessels is to hold the impeller Reynolds number, $Re_d$, constant, that is, to hold constant the normalized fluid velocity at two homologous points of two geometrically similar systems. We calculated the representative viscosity, $\eta$, which is a constitutive factor of $Re_d$, by employing the method proposed by Metzner *et al.*[15, 16, 19] According to this method, $Re_d$ for a pseudoplastic liquid can be calculated from Eq. (5) using the representative shear rate, $\Gamma$, which is linearly proportional to the impeller rotational speed, $n$.

$$Re_d = \frac{\rho n d^2}{\eta_a|_{\Gamma = Bn}} = \rho n d^2 \frac{1 + b(Bn)^c}{a} \tag{5}$$

## 1.2 Calculation conditions

**Figure 1** shows a schematic diagram and analysed region of a stirred vessel fitted with each type of impeller used in this study. The specific dimensions are tabulated

**Table 1.** Dimensions and proportions of each impeller vessel

| Impeller type | | Paddle | Turbine | Anchor |
|---|---|---|---|---|
| Vessel | $H/D$ | 1.0 | 1.0 | 1.0 |
| Impeller location | | | | |
| | $h/D$ | 0.5 | 0.5 | - |
| Impeller | $n_P$ | 6 | 6 | 2 |
| | $d/D$ | 0.5 | 0.5 | 0.9 |
| | $b_h/D$ | - | - | 1.0 |
| | $b_l/D$ | - | 0.125 | - |
| | $b_w/D$ | 0.1 | 0.1 | - |
| | $b_{w1}/D$ | - | - | 0.1 |
| | $b_{w2}/D$ | - | - | 0.1 |
| Shaft | $d_s/D$ | 0.05 | 0.05 | 0.05 |

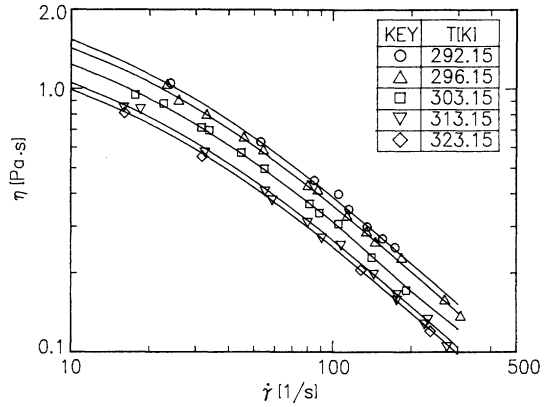


**Fig. 2** Rheological characteristics of 1.2 wt.% aqueous solution of hydroxyethyl cellulose

**Table 2.** Rotational speeds, $n$ [$s^{-1}$], calculated from Eq. (5) when vessels are scaled up at each $Re_d$

| Impeller type | | Paddle | | | Turbine | | | Anchor |
|---|---|---|---|---|---|---|---|---|
| | $Re_d$ | 30 | 60 | 90 | 30 | 60 | 90 | 30 |
| $D/D_0$ = | 1 | 2.51 | 3.81 | 4.83 | 2.67 | 4.08 | 5.18 | 0.94 |
| | 2 | 1.01 | 1.61 | 2.10 | 1.05 | 1.71 | 2.23 | 0.36 |
| | 3 | 0.55 | 0.92 | 1.23 | 0.57 | 0.97 | 1.29 | 0.19 |
| | 4 | 0.35 | 0.60 | 0.82 | 0.36 | 0.63 | 0.85 | 0.12 |

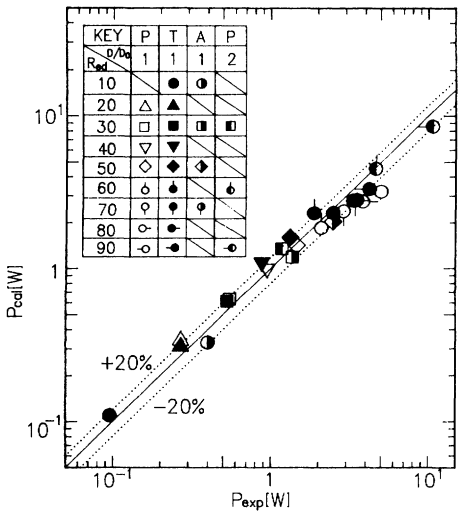


**Fig. 3** Comparison of $P_{cal}$ with $P_{exp}$ in a model vessel equipped with each impeller and in a paddle impeller vessel of 0.4 m diameter at each $Re_d$
(P, T, and A indicate paddle, turbine, and anchor impeller vessel, respectively. Figures from 10 to 90 indicate the values of $Re_d$)

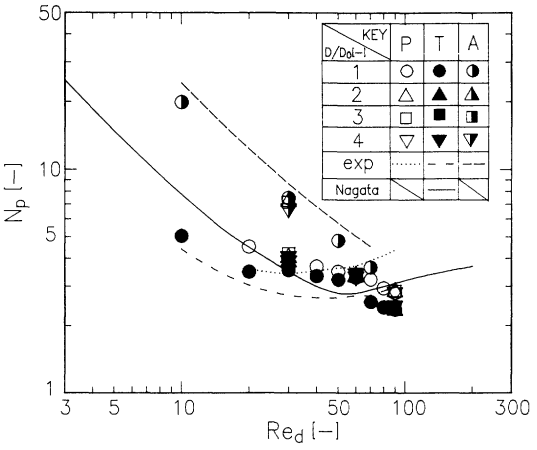


**Fig. 4** $N_{pcal}$-$Re_d$ and $N_{pexp}$-$Re_d$ correlation in each scale vessel with each impeller (Solid line indicates referential curve by Nagata[20])

in **Table 1**. The analysed regions for stirred vessels equipped with a 6-bladed paddle, a 6-bladed turbine, and an anchor impeller are 1/6, 1/6, and 1/2 of the vessel, respectively, due to considerations of the periodic symmetry in the circumferential direction. The number of meshes divided in equal divisions in $r$, $\theta$, and $z$ directions is $20 \times 6 \times 40 = 4800$, $20 \times 6 \times 40 = 4800$, and $20 \times 9 \times 20 = 3600$ in each vessel, through all the calculations, regardless of scale-up ratio[9]. The pseudoplastic liquid taken for the analysis is a 1.2 wt.% aqueous solution of hydroxyethyl cellulose at 20°C.

**Figure 2** shows the rheological characteristics of the liquid at various temperatures measured on a coaxial double cylindrical rheometer. The three constant parameters, $a$, $b$, and $c$, in Eq. (3) have values at 20°C of 2.407 Pa·s, 0.067 $s^c$, and 0.95, respectively. The density, $\rho$, is 1015 kg/$m^3$. The dependency of parameter $a$ on temperature for this liquid is expressed in Eq. (6).

$$a(T) = 2.28 \exp\left(-\frac{0.647(T-296.15)}{38.8+(T-296.15)}\right) \quad (6)$$

The solid lines in Fig. 2 were drawn with Eq. (3) using $a$ ($T$) expressed by Eq. (6). The location for initial injection of solute is in the vicinity of the stirring shaft in the upper half of the liquid, corresponding to about 1.5 vol.% of the whole stirred liquid ($9.42 \times 10^{-5}$ $m^3$ in the case of the model vessel). The diffusion coefficient of solute in the pseudoplastic liquid, $\mathscr{D}$, was set to $1.0 \times 10^{-12}$ $m^2/s$, at which value the diffusive mixing is negligibly small compared with the convective mixing, so that the difference in flow pattern due to the various shapes of impellers is the dominant effect in the mixing process.

We scaled up the model vessel of 0.2 m diameter to

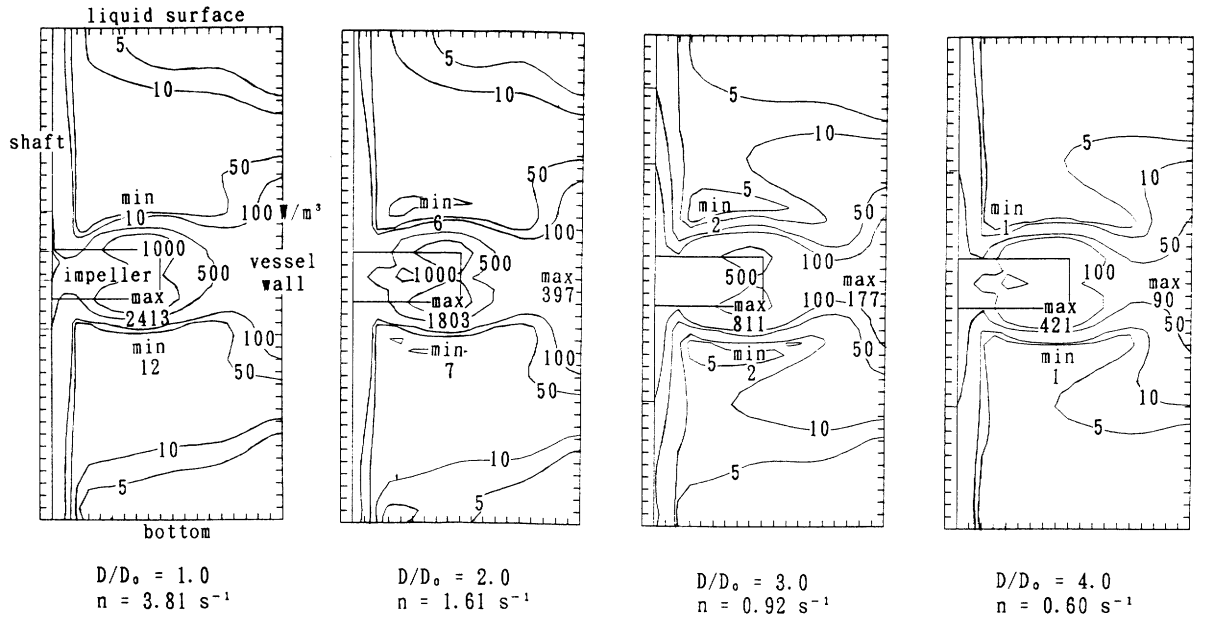


**Fig. 5** (a)

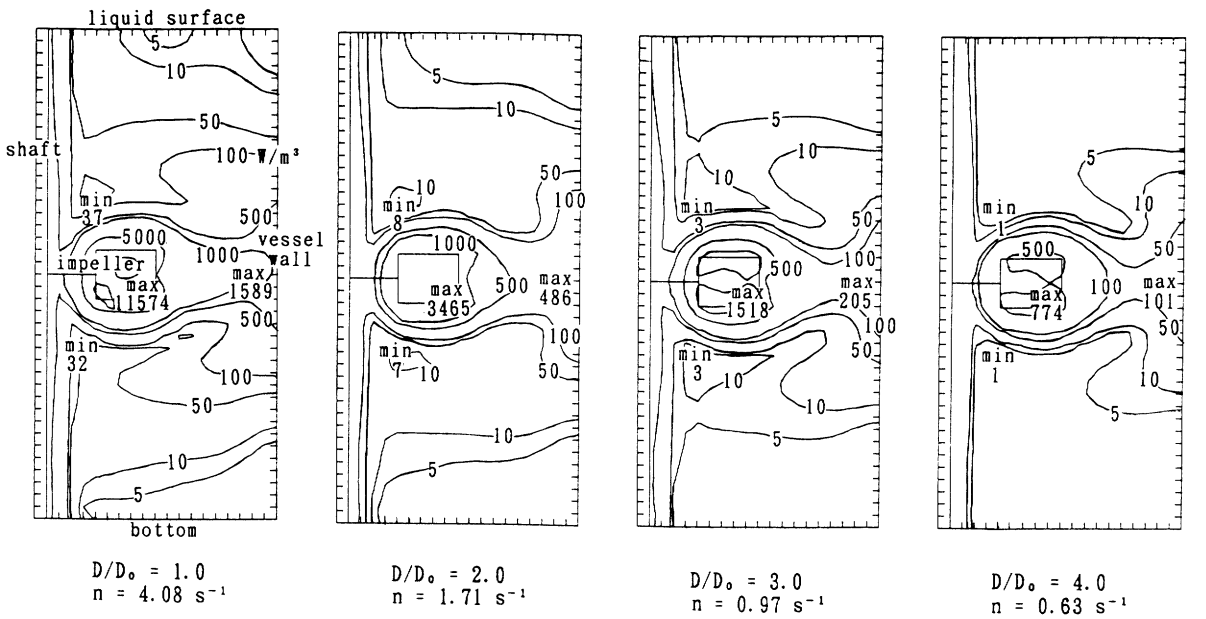


**Fig. 5** (b)

0.8 m in three steps. The values of $Re_d$ held constant were 30, 60, and 90 for the paddle and turbine impellers and 30 for the anchor impeller.

The values of the proportional constant, $B$, in Eq. (5) were set to 13, 11, and 25[19] for paddle, turbine, and anchor impellers, which are used for the two-parameter power law model, assuming that the value of $B$ is not dependent on any physical property of the stirred fluids, that is, on any rheological model, but on the geometry of the stirring impeller[9]. The rotational speeds in scaling-up a stirred vessel with each impeller are tabulated in **Table 2**.

## 2. Results and Discussion

### 2.1 Reliability of power consumption analysis

**Figure 3** shows the verification of numerically calculated results of power consumption, $P_{cal}$, calculated

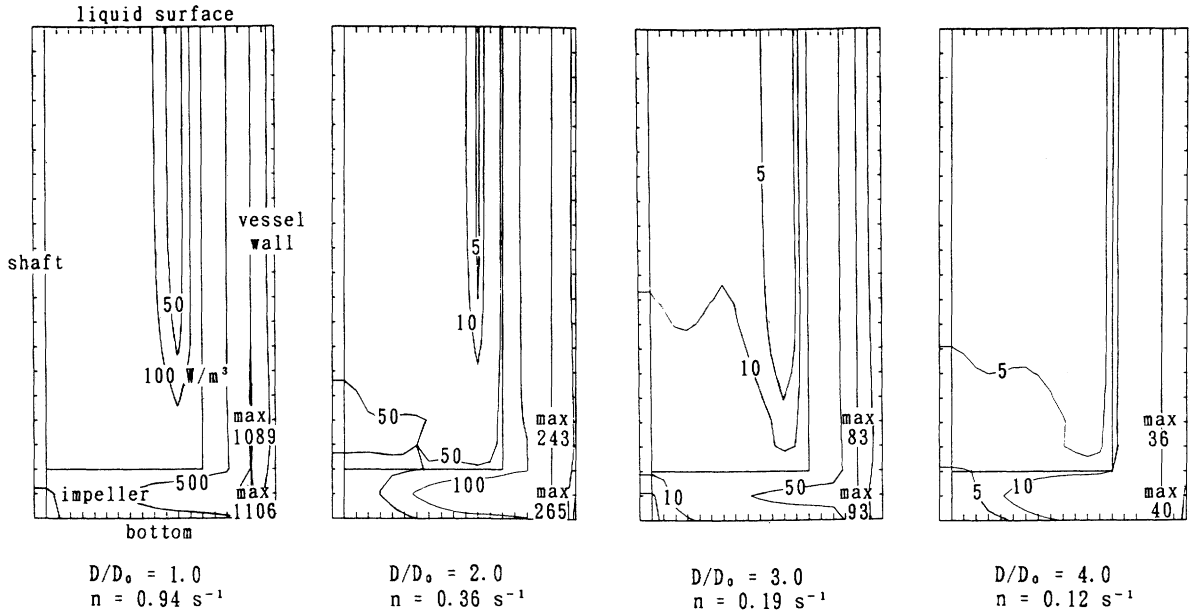


**Fig. 5** (c)

**Fig. 5** Contours of local energy dissipation per unit volume, $p_{Vcal}$, on $r$-$z$ plane in each scale vessel fitted with: (a) paddle impeller at $Re_d = 60$, $J = 4$; (b) turbine impeller at $Re_d = 60$, $J = 4$; (c) anchor impeller at $Re_d = 30$, $J = 5$ (max and min indicate maximum and minimum points, respectively)

from Eq. (1), in a model vessel equipped with each impeller and a 0.4 m diameter vessel with the paddle impeller by comparison with experimental data, $P_{exp}$, based on the measurements of shaft torque by a torquemeter. The rotational speeds, $n$, in the model vessel with each impeller were set so that $Re_d$ varied from 20 to 90 in increments of 10, 10 to 90 in increments of 10, and 10 to 70 in increments of 20, for the paddle, turbine, and anchor impellers respectively. $n$ values were set in the 0.4 m diameter vessel so that $Re_d$ is 30, 60, and 90. Two parallel straight lines in this figure indicate ±20 % relative errors based on the experimental data. Plots are located mostly within the two lines, though $P_{cal}$ shows a tendency to become smaller than $P_{exp}$ where $Re_d$ exceeds 60. This demonstrates that the numerical analysis method has sufficient reliability to estimate the power consumption value, especially in a laminar flow range. Both $P_{cal}$ and $P_{exp}$ values for the paddle and turbine impeller are similar to each other, while those for the anchor impeller are considerably higher than those for the other impellers.

## 2.2 Scaling-up of each impeller vessel

**Figure 4** shows the relation between power number, $N_p$, given by $P/\rho n^3 d^5$, and $Re_d$ for each impeller. Plots indicate simulated results of $N_p$, while several types of lines indicate the experimental data in this work. The solid line indicates a referential curve of the $N_p$-$Re_d$ correlation for a 6-blade turbine for non-Newtonian liquids by Nagata[20]. The $N_p$ values for the turbine, paddle, and anchor impellers at the same $Re_d$ become progressively larger in that order. This tendency can also be observed in the experimental data. The simulated results sufficiently agree with experimental data except for the range of $Re_d > 60$, where $N_p$ begins to increase with $Re_d$, since flow fields start to occupy a transition region. The fact that $N_p$ values simulated in each scaled vessel at $Re_d = 30$, 60, and 90 for the paddle and turbine impeller and at $Re_d = 30$ for the anchor impeller are almost coincident with one another proves the good applicability of the numerical analysis method to scale-up problems.

**Figure 5 (a)**, **(b)**, and **(c)** show $r$-$z$ distributions midway between the adjacent blades ($J = 4$ or 5) of local viscous dissipation energy per unit volume, $p_v$, that is $\gamma^2 \cdot \eta_a$, in each scale vessel with the paddle and turbine impeller at $Re_d = 60$, and with the anchor impeller at $Re_d = 30$, respectively. Flow patterns are very similar to each other for the paddle and turbine impeller as reported previously[8-10]. The distributions of $p_V$ for the two impellers are also similar, that is, the larger part of the energy provided by the impeller is consumed in the vicinity of the impeller, and the ridge lines of the $p_V$ contours coincide with the location of the discharge flow from the impellers and the circulation flows in both halves of the vessels. The power for the turbine impeller, however, is consumed more locally around the impeller than for the paddle impeller. In comparison with this, the power consumption for the anchor impeller is comparatively uniform in the whole of the vessel, since forced convective

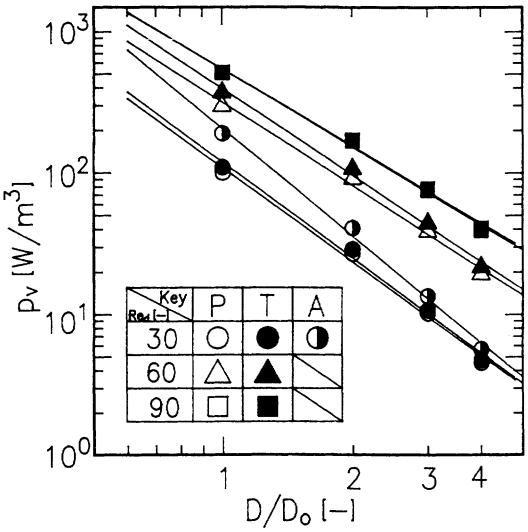


**Fig. 6** Relation between $P_{Vcal}$ and scale-up ratio in each impeller vessel at each $Re_d$

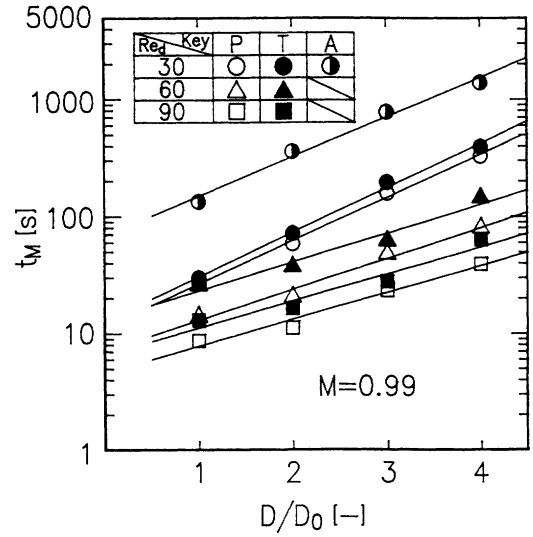


**Fig. 7** Relation between mixing time, $t_{Mcal}$, and scale-up ratio in each impeller vessel at each $Re_d$

flows are created in the vicinity of the side wall and bottom of the vessel by the larger impeller[8-10]. As shown in Table 2, when we scale-up a stirred vessel while holding $Re_d$ constant, the rotational speeds of the impeller decrease with an increase in the scale-up ratio, $D/D_0$, and the shear rates, $\dot{\gamma}$, in the vessel decrease therewith. Consequently, the distribution of $p_V$ decreases with an increase in $D/D_0$, although the apparent viscosity of the pseudoplastic liquid increases with a decrease in the shear rate, as shown in Fig. 2.

**Figure 6** shows the relation between power consumption per unit volume, $P_V$, given by $P_{cal}/V_{tot}$, and scale-up ratio for the three types of impellers at $Re_d = 30$, 60, and 90. $P_V$ decreases with an increase in the scale-up ratio at the same $Re_d$, expressed as follows:

$$P_V = \alpha \cdot (D/D_0)^{-\beta} \tag{7}$$

$P_V$ values in the paddle and turbine impeller vessels almost coincide again, like $P$, mentioned above. $P_V$ for the anchor impeller of the model scale is, however, higher than that for the other types of impellers since the apparent viscosity in the anchor model vessel is higher than that in the others because of the lower rotational speed due to the larger impeller diameter and the larger $B$ value. $P_V$, however, decreases with an increase in $D/D_0$ more rapidly than the other impeller vessels, since the apparent viscosity is high, near the zero shear viscosity even in the model vessel, and so the reduction effect of shear rate is more dominant in the larger-scale vessels. Figure 6 can also be used to estimate rotational speeds when we scale up a stirred vessel while holding $P_V$ constant, by determining $Re_d$ from $P_V$, and $D/D_0$ by interpolation of this figure and solving for $n$ in Eq. (5).

**Figure 7** shows the relation between mixing time, $t_M$, and scale-up ratio in the three types of impeller vessels. $t_M$ increases exponentially with an increase in $D/D_0$* expressed as the following equation:

$$t_M = \gamma \cdot \exp_{10}((D/D_0) \cdot \delta) \tag{8}$$

The reasons why $t_M$ in the paddle, turbine, and anchor impeller vessels become progressively larger in this order are that the mixing between the upper and lower halves of the vessel in the turbine impeller vessel is obstructed by a disc plate at the center of the vessel and that the mixing in the anchor impeller mixer is rather bad owing to lack of longitudinal flow in the upper part of the vessel[8, 10].

**Figure 8** shows the relation between $E_M$ in the three impeller vessels and the scale-up ratio. $E_M$ increases with an increase in $D/D_0$ at the same $Re_d$, expressed as follows:

$$E_M = \varepsilon \cdot (D/D_0)^{\zeta} \tag{9}$$

$E_M$ values in the paddle, turbine, and anchor impeller vessels become progressively larger, again in that order. This is attributable to the influence of $t_M$ in each impeller vessel.

**Table 3** summarizes the correlation equations of $P_V$, $t_M$, and $E_M$ at each $Re_d$ value with scale-up ratio for stirred vessels equipped with the three types of impellers. It is worth noting that $\beta$ is nearly equal to 2 at $Re_d = 60$, where $\eta^2 \cdot n$ is approximately constant on Fig. 2, as expected in the laminar region (See Appendix).

## Conclusions

We proposed a numerical analysis method of estimating power consumption in certain kinds of plate impeller vessels for a highly viscous pseudo plastic

* We have already reported the reliability of estimation for $t_M$ in the model-scale vessel[8, 10]. Regarding large-scale vessels, we ascertained the good reliability (within 20 % relative error) in the 0.4 m vessel with the paddle impeller by observing the non-uniformity of the solute concentration using Fluorescein Sodium as a tracer reagent on the $r$-$z$ slit-light plane[11, 12].

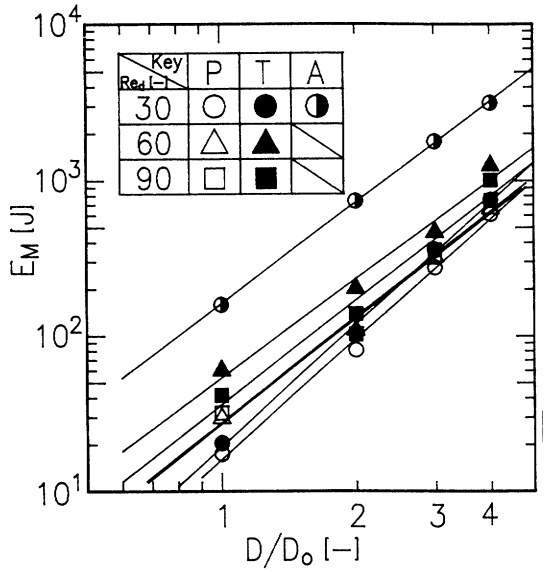


**Fig. 8** Relation between mixing energy, $E_{Mcal}$, and scale-up ratio in each impeller vessel at each $Re_d$

liquid. The reliability of the method was ascertained by verifying numerically calculated results by comparison with experimental data from a torque-meter. Subsequently, we applied the method to paddle, turbine, and anchor impeller vessels of 0.2 to 0.8 m diameters with geometrical symmetry and numerically investigated the scale-up effect on power consumption and mixing time in each vessel. It was found from these analyses that the numerical analysis method presented here is an effective means of quantitatively anticipating the relation between power consumption, mixing time, or mixing energy, and scale-up ratio of a pseudo plastic liquid in impeller vessels of each shape.

### Appendix

$P_V$ is proportional to $N_p{\cdot}\rho\, n^3 d^2$. Further, $P_V$ is transformed to Eq. (A-1) in the laminar region, since $N_p{\cdot}Re_d$ is constant in that region and $Re_d$ is $\rho\, nd^2/\eta$.

$$P_V \propto \eta^2 n \cdot Re_d / \rho d^2 = \eta n^2 \qquad \text{(A-1)}$$

From Eq. (A-1) and the fact that $D$ is proportional to $d$, the value of $\beta$ in Eq. (7) is expected to be 2, where $\eta^2 n$ is constant when we scale-up a vessel while holding $Re_d$ constant. $\beta$ is expected to be 0, where $\eta n^2$ is constant, in which case both the shear rate field and the $Re_d$ region are higher in value than the region mentioned above, as found in Fig. 2.


### Acknowledgments

The authors are grateful to Mr. T. Nozawa, of Toshiba Corp., Mr. M. Kato, of RICOH Co., Ltd., Mr. M. Fujita, of Fuji Xerox Co., Ltd., Mr. T. Asotani, and Ms. T. Kimura for contributing to the present work. The numerical calculations were carried out using the HITAC M-680 and S-820/80 of the Computer Center, University of Tokyo.


### Nomenclature

| | | | |
|---|---|---|---|
| $a$ | = | viscosity constitutive equation parameter, defined by Eq. (6) | [Pa·s] |
| $B$ | = | constant value for calculation of $\Gamma$ | [-] |
| $b$ | = | viscosity constitutive equation parameter in Eq. (3) | [$s^c$] |
| $b_h$ | = | blade height of an anchor impeller | [m] |
| $b_l$ | = | blade length of a turbine impeller | [m] |
| $b_w$ | = | blade width | [m] |
| $b_{w1}$ | = | blade width of an anchor impeller | [m] |
| $b_{w2}$ | = | blade width of an anchor impeller | [m] |
| $C$ | = | concentration of solution normalized by injected solute moles | [$m^{-3}$] |
| $C_m$ | = | normalized mean concentration | [$m^{-3}$] |
| $C_0$ | = | normalized initial concentration | [$m^{-3}$] |
| $C^*$ | = | dimensionless concentration, defined by Eq. (4) | [-] |
| $c$ | = | viscosity constitutive equation index in Eq. (3) | [-] |
| $D$ | = | inside diameter of vessel | [m] |
| $D_0$ | = | inside diameter of a model vessel | [m] |
| $\mathscr{D}$ | = | diffusion coefficient of solute | [$m^2/s$] |
| $d$ | = | impeller diameter | [m] |
| $d_s$ | = | impeller shaft diameter | [m] |
| $E_M$ | = | energy required to attain mixing | [J] |
| $H$ | = | liquid height | [m] |
| $h$ | = | impeller height | [m] |
| $I$ | = | mesh number in $r$-direction | [-] |
| $J$ | = | mesh number in $\theta$-direction | [-] |
| $K$ | = | mesh number in $z$-direction | [-] |
| $M$ | = | degree of mixing attained | [-] |
| $N_p$ | = | power number | [-] |
| $n$ | = | rotational speed of impeller | [$s^{-1}$] |
| $n_p$ | = | number of impeller blades | [-] |
| $P$ | = | power consumption in a whole vessel | [W] |
| $P_{cal}$ | = | $P$ value calculated according to Eq. (1) | [W] |
| $P_{exp}$ | = | $P$ value based on the experimental data of shaft torque | [W] |
| $P_V$ | = | power consumption per unit volume | [$W/m^3$] |
| $p_V$ | = | local value of $P_V$ | [$W/m^3$] |
| $Re_d$ | = | impeller Reynolds number, defined by Eq. (5) | [-] |
| $r$ | = | radius | [m] |
| $T$ | = | temperature | [K] |
| $t_M$ | = | mixing time | [s] |
| $V$ | = | volume | [$m^3$] |
| $V_{tot}$ | = | total volume of a stirred liquid | [$m^3$] |
| $z$ | = | height | [m] |
| $\alpha$ | = | correlative equation parameter in Eq. (7) and in Table 3 | [$W/m^3$] |
| $\beta$ | = | correlative equation parameter in Eq. (7) and in Table 3 | [-] |
| $\Gamma$ | = | representative shear rate in a stirred vessel | [$s^{-1}$] |

**Table 3.** Correlative equations between $P_V, t_M, E_M$, and scale-up ratio, $D/D_0$

| Impeller type | Paddle | | Turbine | | Anchor | |
|---|---|---|---|---|---|---|
| $P_V = \alpha \cdot (D/D_0)^{-\beta}$ [$W/m^3$]; | $\alpha$ | $\beta$ | $\alpha$ | $\beta$ | $\alpha$ | $\beta$ |
| $Re_d$ = 30 | 108.3 | 2.20 | 118.8 | 2.24 | 204.7 | 2.51 |
| 60 | 315.0 | 1.95 | 393.6 | 2.03 | - | - |
| 90 | 542.5 | 1.81 | 541.2 | 1.83 | - | - |
| $t_M = \gamma \cdot \exp_{10}((D/D_0) \cdot \delta)$ [s]; | $\gamma$ | $\delta$ | $\gamma$ | $\delta$ | $\gamma$ | $\delta$ |
| $Re_d$ = 30 | 11.87 | 0.365 | 12.81 | 0.379 | 68.23 | 0.339 |
| 60 | 8.45 | 0.251 | 13.22 | 0.246 | - | - |
| 90 | 5.11 | 0.222 | 6.60 | 0.231 | - | - |
| $E_M = \varepsilon \cdot (D/D_0)^{\zeta}$ [J]; | $\varepsilon$ | $\zeta$ | $\varepsilon$ | $\zeta$ | $\varepsilon$ | $\zeta$ |
| $Re_d$ = 30 | 16.19 | 2.57 | 19.44 | 2.61 | 161.8 | 2.17 |
| 60 | 27.27 | 2.25 | 53.93 | 2.12 | - | - |
| 90 | 27.92 | 2.26 | 36.29 | 2.23 | - | - |

| | | | |
|---|---|---|---|
| $\gamma$ | = | correlative equation parameter in Eq. (8) and in Table 3 | [s] |
| $\dot{\gamma}$ | = | shear rate | [$s^{-1}$] |
| $\Delta$ | = | increment of mesh | [-] |
| $\boldsymbol{\Delta}$ | = | deformation rate tensor | [$s^{-1}$] |
| $\delta$ | = | correlative equation parameter in Eq. (8) and in Table 3 | [-] |
| $\varepsilon$ | = | correlative equation parameter in Eq. (9) and in Table 3 | [J] |
| $\zeta$ | = | correlative equation parameter in Eq. (9) and in Table 3 | [-] |
| $\eta$ | = | representative viscosity in a stirred vessel | [Pa·s] |
| $\eta_a$ | = | apparent viscosity expressed by Eq. (3) | [Pa·s] |
| $\theta$ | = | angle | [rad] |
| $\rho$ | = | density | [$kg/m^3$] |

<Subscripts>

| | | |
|---|---|---|
| *cal* | = | calculated |
| *exp* | = | experimental |

**Literature Cited**


1) Bakker, A.: Ph. D. Thesis, Tech. Univ. Delft (1992)
2) Bertrand, J. and J.P. Couderc: *Chem. Eng. Res. Des.*, **63**, 259-263 (1985)
3) Bertrand, J.: Proceedings of 4th World Congress of Chemical Engineering, pp. 753-771 (1991)
4) Hiraoka, S., I. Yamada and K. Mizoguchi: *J. Chem. Eng. Japan*, **11**, 487-493 (1978)
5) idem, ibid, **12**, 56-62 (1979)
6) Hiraoka, S., I. Yamada, T. Aragaki, H. Nishiki, A. Sato and T. Takagi: *J. Chem. Eng. Japan*, **21**, 79-86 (1988)
7) Kaminoyama, M., F. Saito and M. Kamiwano: *Kagaku Kogaku Ronbunshu*, **14**, 786-793 (1988); English translation in Intl. Chem. Engng., **30**, 720-728 (1990)
8) Kaminoyama, M., F. Saito and M. Kamiwano: Proceedings of AIChE 1989 Annual Meeting, e-115 (1989)
9) Kaminoyama, M., F. Saito and M. Kamiwano: *J. Chem. Eng. Japan*, **23**, 214-221 (1990)
10) Kaminoyama, M., F. Saito and M. Kamiwano: *Kagaku Kogaku Ronbunshu*, **16**, 820-829 (1990)
11) Kamiwano, M., T. Koga and K. Ohya: *Kagaku Kogaku Ronbunshu*, **5**, 520-525 (1979)
12) Kamiwano, M., K. Ohya and T. Koga: *Kagaku Kogaku Ronbunshu*, **5**, 537-539 (1979)
13) Kamiwano, M., F. Saito and M. Kaminoyama: *Kagaku Kogaku Ronbunshu*, **14**, 316-322 (1988); English translation in Intl. Chem. Engng., **30**, 274-280 (1990)
14) Kresta, S.M. and P.E. Wood: *AIChE J.*, **37**, 448-460 (1991)
15) Metzner, A.B. and R.E. Otto: *AIChE J.*, **3**, 3-10 (1957)
16) Metzner, A.B., R.H. Feehs, H.L.. Ramos, R.E. Otto and J.D. Tuthill: *AIChE J.*, **7**, 3-9 (1961)
17) Middleton, J.C., F. Pierce and P.M. Lynch: *Chem. Eng. Res. Des.*, **64**, 18-22 (1986)
18) Mitsuishi, N. and N. Hirai: *J. Chem. Eng. Japan*, **2**, 217-224 (1969)
19) Nagata, S., M. Nishikawa, H. Tada and S. Gotoh: *J. Chem. Eng. Japan*, **4**, 72-76 (1971)
20) Nagata, S.: "Mixing Principles and Applications", p.81 Kodansha Ltd., Japan, (1975)
21) idem, ibid, p. 139 (1975)
22) Ohta, M., M. Kuriyama, K. Arai and S. Saito: *J. Chem. Eng. Japan*, **18**, 81-84 (1985)
23) Placek, J., L.L. Tavlarides, G.W. Smith and I. Fort: *AIChE J.*, **32**, 1771-1786 (1986)
24) Spragg, A.J.P., S.J. Maskell and M.A. Patrick: Proceedings of 5th European Conference on Mixing, pp. 507-514 (1985)
25) Weetman, R.J.: Proceedings of 7th European Congress on Mixing, pp. 25-32 (1991)
26) Williams, M.L., R.F. Landel and J.D. Ferry: *J. Amer. Chem. Soc.*, **77**, 3701-3707 (1955)